Updated comments on projector augmented wave (PAW) implementations within various electronic structure code packages

N.A.W. Holzwarth

Department of Physics, Wake Forest University, Winston-Salem,, NC 27109, USA

ARTICLE INFO

ABSTRACT

The projector augmented wave (PAW) formalism of Blöchl (1994) has been implemented in a number of electronic structure code packages and generally has become an important tool for density functional simulations of materials. However, it is occasionally possible to obtain unphysical results. A source for such occasional anomalous behavior is traced to one contribution present in some codes that use the reformulation of the exchange–correlation terms introduced by Kresse et al. (1999). A remedy is discussed which has been implemented in new versions of the atomic dataset generation program ATOMPAW (Holzwarth et al. 2001).

© 2019 Elsevier B.V. All rights reserved.

1. Introduction

This short paper presents an update to a paper (Paper 1) written several years ago [1] concerning the implementation of the Projector Augmented Wave (PAW) formalism developed by Blöchl [2] within different open source electronic structure code packages based on density functional theory [3,4]. In fact, the community of computational condensed matter research has benefited enormously from the work of the developers who maintain high quality public domain software for density functional electronic structure calculations. For example, we use the ABINIT [5] and the QUANTUM ESPRESSO [6] packages interchangeably for structural and energy simulations with the help of atomic datasets generated by our ATOMPAW [7] code.

In Paper 1, we noted that the original Blöchl PAW formalism for evaluating the exchange–correlation contributions to the Kohn–Sham equations is numerically well-behaved, while the corresponding implementation introduced by Kresse [8] can exhibit some numerical difficulties. In the present paper, additional surprising numerical difficulties are analyzed for the Kresse formulation.

2. Formalism

The detailed formalism was presented in Paper 1. Here we only repeat the main points. Blöchl's expression for evaluating the exchange–correlation energy is given by

$$E_{xc}^{B} = E_{xc}[\tilde{n} + \tilde{n}_c] + \sum_a \left(E_{xc}[n^a + n_c^a] - E_{xc}[\tilde{n}^a + \tilde{n}_c^a] \right). \quad (1)$$

Kresse's expression for evaluating the exchange–correlation energy is given by

$$E_{xc}^{K} = E_{xc}[\tilde{n} + \tilde{n}_c + \hat{n}] + \sum_a \left(E_{xc}[n^a + n_c^a] - E_{xc}[\tilde{n}^a + \tilde{n}_c^a + \hat{n}^a] \right). \quad (2)$$

Here, the notation $E_{xc}[n]$ denotes the evaluation of the chosen exchange–correlation functional (such as LDA [9], PBE [10], PBESOL [11], etc. [12]) as a function of the density argument $n(\mathbf{r})$. There are several contributions to the density arguments in these expressions. The notation $\tilde{n}$ denotes the valence electron pseudodensity evaluated in a plane wave basis or corresponding real-space grid. The notation $\tilde{n}_c$ denotes the core pseudodensity function following the non-linear core correction introduced by Louie et al. [13] which is also evaluated in a plane wave basis or corresponding real-space grid. By construction, the pseudodensity functions accurately represent the physical valence electron density outside of spheres of radius r_c^a centered on each atom. The contributions from summations over that atom centered terms for each atom a are evaluated on atom-centered grids. By construction, for each atom a, the expressions $\left(E_{xc}[n^a + n_c^a] - E_{xc}[\tilde{n}^a + \tilde{n}_c^a] \right)$ in the Blöchl formulation or $\left(E_{xc}[n^a + n_c^a] - E_{xc}[\tilde{n}^a + \tilde{n}_c^a + \hat{n}^a] \right)$ in the Kresse formulation vanish outside a sphere of radius r_c^a. These include the valence density n^a represented in terms of all-electron atomic basis functions and the corresponding valence pseudodensity $\tilde{n}^a$ represented in terms of atomic pseudobasis functions. Also included are the full core density n_c^a and the corresponding pseudocore density $\tilde{n}_c^a$, where

$$\tilde{n}_c(\mathbf{r}) \equiv \sum_a \tilde{n}_c^a \left(|\mathbf{r} - \mathbf{R}^a| \right), \quad (3)$$

with $\mathbf{R}^a$ denoting the coordinate of the atom center a [14]. Additionally, the Kresse formulation includes the valence
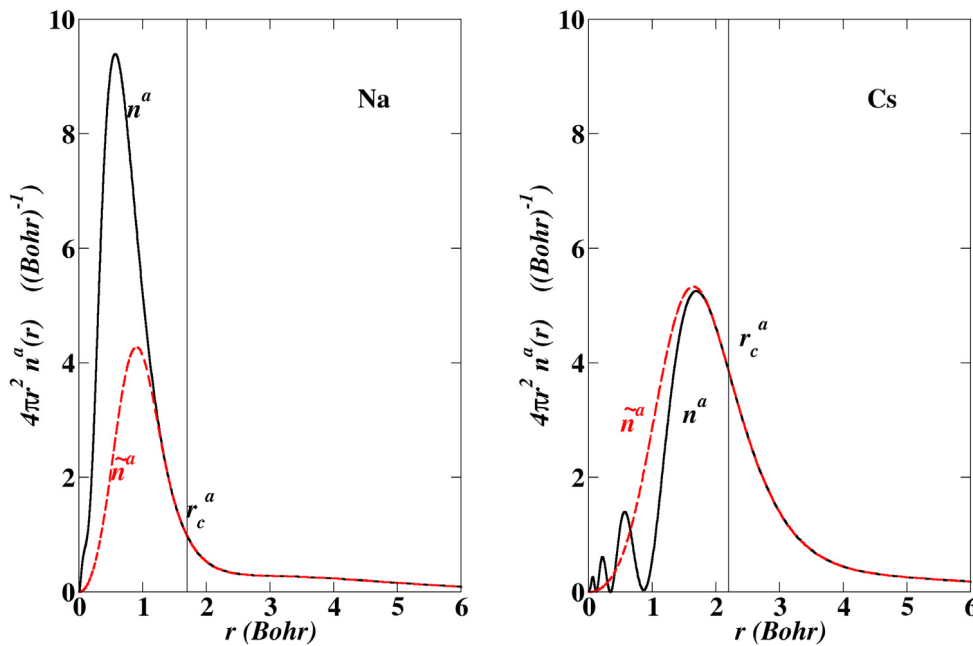
E-mail address: natalie@wfu.edu.

Fig. 1. Plot of valence electron density ($n^a(r)$) and pseudodensity ($\tilde{n}^a(r)$) for Na (left) and Cs (right).

compensation charge density as a summation of atom centered terms:

$$\hat{n}(\mathbf{r}) = \sum_a \hat{n}^a(\mathbf{r} - \mathbf{R}^a). \tag{4}$$

The compensation charge density was introduced by Blöchl in order to ensure that the multipole moments of the Hartree energy are calculated correctly and is similar to the augmentation function $Q(\mathbf{r})$ introduced in the ultrasoft pseudopotential formalism [15–17]. The compensation charge density does not logically belong in the evaluation of the exchange–correlation functional. As noted in Paper 1, its presence in codes that use the Kresse formulation of Eq. (2) often cancels out of the final result, but in some cases, the sensitivity of the exchange–correlation functional to the shape of density can introduce errors. Since the publication of Paper 1, the ABINIT code was modified in 2010 (Version 6.2) to use the same exchange–correlation form as used within the dataset generation program which is by default the Blöchl form for ATOMPAW to generate atomic datasets for ABINIT. However some other code packages, such as QUANTUM-ESPRESSO [6] and VASP [8,18] still exclusively use the Kresse formulation.

In the course of our routine studies of a variety of materials, what we have newly realized is that *when the compensation charge is negative in some regions of space, the Kresse formulation can give quite surprising results*, because of the possibility that the argument of the exchange–correlation functional may be negative.

Accordingly, we have modified our ATOMPAW code to create modified atomic datasets which are more likely to give reasonable results for the Kresse formalism. That is, the ATOMPAW code (Version $\geq$ 4.1.0.4) now creates a dataset for use with the Kresse form of the exchange–correlation contributions only if

$$\tilde{n}_c^a(r) + \hat{n}^a(r) \geq 0 \quad \text{for} \quad 0 \leq r \leq r_c^a. \tag{5}$$

For the examples we have encountered so far, the inequality (5) can be achieved by increasing the magnitude of the smoothed core density $\tilde{n}_c^a(r)$ by reducing the matching radius (r_{core} in the ATOMPAW input file) which is used to construct the core pseudodensity [7,13]. It is also sometimes necessary to slightly adjust the shape or extent of the compensation charge function $\hat{n}^a(r)$. These

adjustments ensure that the datasets prepared for use in codes that use the Kresse formulation of the exchange–correlation functional have continuous local pseudopotentials and that it is less likely that negative density arguments within the exchange–correlation functionals will be encountered within the full materials simulations. Of course, the adjustments may affect the convergence properties of the dataset which should always be checked.

It is our understanding that the developers of the VASP code are aware of this problem and have implemented a positive density correction similar to that described by Eq. (5). The developers of the QUANTUM ESPRESSO code are also aware of this problem and in a publication [19] describing their pseudopotential generation code (called *ld1*) the notion of a positive compensation charge is mentioned as a guiding principle.

3. Examples

Unless care is taken to avoid it, the occurrence of negative values of the compensation charge density within the PAW formalism seems to be more common than one might expect. For a spherical atom in its ground state configuration, the valence compensation charge density can be written in the form

$$\hat{n}^a(r) = q_{\text{eff}}^a s(r), \tag{6}$$

where

$$q_{\text{eff}}^a \equiv \int_{r \leq r_c^a} d^3 r \left(n^a(\mathbf{r}) - \tilde{n}^a(\mathbf{r}) \right), \tag{7}$$

and where $s(r)$ is a spherically symmetric density shape function confined within a sphere of radius r_c^a and normalized to unity. Typically, the shape function $s(r)$ is chosen to be positive definite, so that the sign of $\hat{n}^a(r)$ is controlled by the sign of q_{eff}^a.

The sign of q_{eff}^a depends both on the choice of the partitioning between core and valence electron treatments and on the choice of the pseudopotential radius r_c^a. For example, we examine the cases of Na, P, S, Cl, Br, and Cs. For this study, we used the local density approximation (LDA) [9]; very similar results were obtained using the PBESOL exchange–correlation form [11]. The parameters for generating the atomic datasets using ATOMPAW
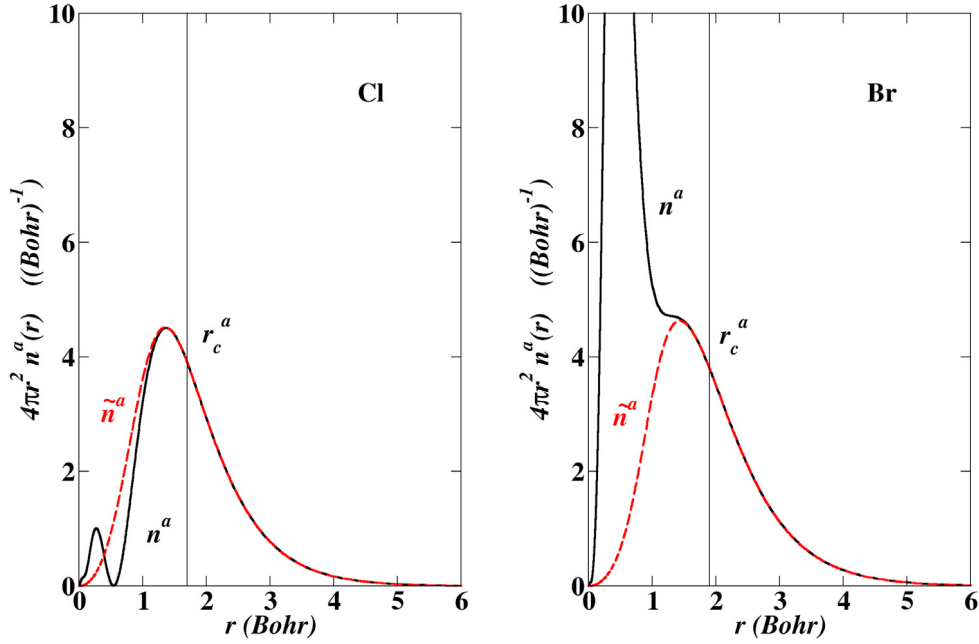
Fig. 2. Plot of valence electron density ($n^a(r)$) and pseudodensity ($\tilde{n}^a(r)$) for Cl (left) and Br (right).

Table 1

Compensation charges q^a_{eff} as defined by Eq. (7) for various ground state atoms, listing the core and valence configurations, the pseudopotential radius r^a_c in Bohr units, and the value of q_{eff} calculated using Eq. (7).

Atom	Core	Valence	r^a_c	q^a_{eff}
Na	[He]	$2s^2 2p^6 3s^1$	1.7	3.88
P	[Ne]	$3s^2 3p^3$	1.7	−0.19
S	[Ne]	$3s^2 3p^4$	1.7	−0.35
Cl	[Ne]	$3s^2 3p^5$	1.7	−0.44
Br	[Ar]	$3d^{10} 4s^2 4p^5$	1.9	8.79
Cs	[Kr] $4d^{10}$	$5s^2 5p^6 6s^1$	2.2	−1.07

Fig. 3. Binding energy curve of CsBr, plotting energy (eV) relative to the equilibrium value versus cubic lattice constant a (Å). Compared are results computed with the linearized augmented plane wave approach [21] using the WIEN2k package [22] with PAW results generated with either Blöchl's or Kresse's formulation of the exchange–correlation terms, using the ABINIT (AB) or QUANTUM ESPRESSO (QE) codes, and corrected or not corrected following Eq. (5), as indicated. The binding energy calculations were generated by using an energy cut off of 64 Ry.

were taken from our current and previous materials studies. Most of the dataset parameters are derived from datasets generated by Jollet et al., [20] optimized to agree with all electron binding energy curves of representative binary compounds. The results are summarized in Table 1. These results show that the occurrence of negative compensation charges is not particularly rare.

3.1. Example plots of the valence electron densities and pseudodensities

In order to better understand the origin of the positive and negative compensation charges q^a_{eff}, we show plots of $n^a(r)$ and $\tilde{n}^a(r)$ for some of the examples. In these examples, the shapes of the pseudodensities for $0 \leq r \leq r^a_c$ are quite variable as is the sign of q^a_{eff}. Results for Na and Cs are shown in Fig. 1 and for Cl and Br are shown in Fig. 2, respectively.

3.2. Example binding energy plots

In Fig. 3 we show the results of computing the total electronic energy as a function of lattice constant for CsBr, comparing the all-electron calculation results generated using the linearized augmented wave formulation [21] as implemented in the WIEN2k package [22], the various formulations of the PAW approach discussed here using the ABINIT and QUANTUM ESPRESSO codes with datasets generated with ATOMPAW using parameters listed in Table 1. The dataset generated without the positive density correction mentioned in Eq. (5), gives a binding energy curve in
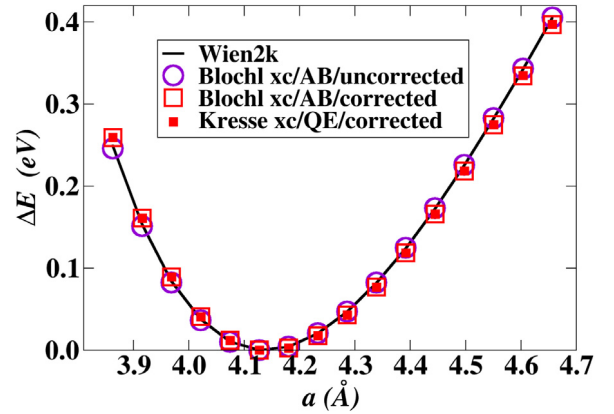
excellent agreement with the WIEN2k result using the ABINIT code with the Blöchl exchange–correlation form, while no binding energy results could be obtained using the QUANTUM ESPRESSO code with the Kresse exchange–correlation form. However, by modifying the dataset according to the positive density correction (Eq. (5)), the results are essentially identical for both ABINIT and QUANTUM ESPRESSO and very close to the WIEN2k results and to the PAW results generated by ABINIT by the uncorrected dataset.

3.3. Example phonon density of states

A somewhat more subtle manifestation of the effects of negative compensation charge in the Kresse formulation of the exchange–correlation functional comes in the evaluation of the lattice vibrational spectrum using density functional perturbation
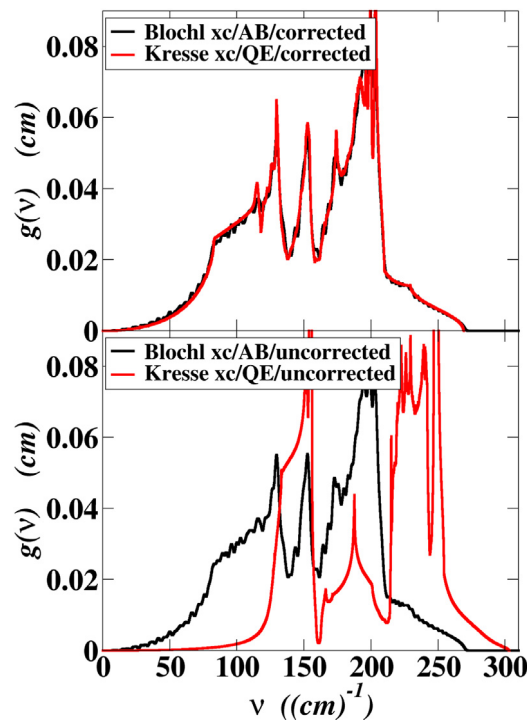
Fig. 4. Plots of the densities of phonon modes $g(\nu)$, normalized to 6 when integrated over wavenumber ν, calculated for a unit cell of NaCl at equilibrium. Compared are results calculated with PAW datasets using either Blöchl's or Kresse's formulation of the exchange–correlation terms, using the ABINIT (AB) or QUANTUM ESPRESSO (QE) codes, and corrected or not corrected following Eq. (5), as indicated.

theory [23]. As an example, the binding energy curves for NaCl using uncorrected atomic datasets and the Blöchl and Kresse expressions were in good agreement; the surprise came in evaluating the phonon spectrum. Fig. 4 shows that for NaCl, results for the vibrational density function $g(\nu)$ are insensitive to the positive density correction when the Blöchl form of the exchange–correlation function is used. However, results for $g(\nu)$ are drastically modified when the Kresse form of the exchange–correlation function is used without the positive density correction.

4. Summary and conclusions

Hopefully this discussion has presented useful insight into the construction of numerically stable PAW datasets. The positive density correction given in Eq. (5) has restored the possibility of using equivalent atomic datasets generated by ATOMPAW in both ABINIT and QUANTUM ESPRESSO for electronic structure simulations. It is rather alarming that this issue remained hidden from our notice as developers of the ATOMPAW code for so many years. In fact, PAW datasets generated by earlier versions of the ATOMPAW code should be used in QUANTUM ESPRESSO with caution. The examples considered in this study focused on ground state and density functional perturbation theory calculations. However, one expects that other calculations that depend on the exchange–correlation functional may also be affected.

The following comments summarize details of the effects of negative compensation charge on the Kresse form of the exchange–correlation PAW functional. The exchange–correlation functionals are not defined for negative arguments, but most codes return values of zero for the energy and potential values. Within the ATOMPAW code, this would be encountered in the preparation of the unscreened local potential appropriate for use in the Kresse formulation, and would result in radially discontinuous unscreened local potential functions at the radii where the effective density changes sign. Within the corresponding materials calculations using the Kresse formulation, the code not

only must deal with discontinuous local potentials, but one also expects that for the given choice of pseudization parameters, negative density arguments may appear throughout the computation. Fortunately, the positivity correction (Eq. (5)) seems to provide a reliable fix for the problem.

References

[1] M. Torrent, N.A.W. Holzwarth, F. Jollet, D. Harris, N. Lepley, X. Xu, Comput. Phys. Comm. 181 (2010) 1862–1867, http://dx.doi.org/10.1016/j.cpc.2010.07.06.
[2] P.E. Blöchl, Phys. Rev. B 50 (1994) 17953–17979.
[3] P. Hohenberg, W. Kohn, Phys. Rev. 136 (1964) B864–B871.
[4] W. Kohn, L.J. Sham, Phys. Rev. 140 (1965) A1133–A1138.
[5] X. Gonze, F. Jollet, F.A. Araujo, D. Adams, B. Amadon, T. Applencourt, C. Audouze, J.-M. Beuken, J. Bieder, A. Bokhanchuk, E. Bousquet, F. Bruneval, D. Caliste, M. Côté, F. Dahm, F.D. Pieve, M. Delaveau, M.D. Gennaro, B. Dorado, C. Espejo, G. Geneste, L. Genovese, A. Gerossier, M. Giantomassi, Y. Gillet, D.R. Hamann, L. He, G. Jomard, J.L. Janssen, S.L. Roux, A. Levitt, A. Lherbier, F. Liu, I. Lukačević, A. Martin, C. Martins, M.J.T. Oliveira, S. Poncé, Y. Pouillon, T. Rangel, G.-M. Rignanese, A.H. Romero, B. Rousseau, O. Rubel, A.A. Shukri, M. Stankovski, M. Torrent, M.J.V. Setten, B.V. Troye, M.J. Verstraete, D. Waroquiers, J. Wiktor, B. Xu, A. Zhou, J.W. Zwanziger, Comput. Phys. Comm. 205 (2016) 106–131, http://dx.doi.org/10.1016/j.cpc.2016.04.003, URL http://www.sciencedirect.com/science/article/pii/S0010465516300923.

[6] P. Giannozzi, O. Andreussi, T. Brumme, O. Bunau, M. Buongiorno Nardelli, M. Calandra, R. Car, C. Cavazzoni, D. Ceresoli, M. Cococcioni, N. Colonna, I. Carnimeo, A. Dal Corso, S. de Gironcoli, P. Delugas, R.A. DiStasio, A. Ferretti, A. Floris, G. Fratesi, G. Fugallo, R. Gebauer, U. Gerstmann, F. Giustino, T. Gorni, J. Jia, M. Kawamura, H.-Y. Ko, A. Kokalj, E. Küçükbenli, M. Lazzeri, M. Marsili, N. Marzari, F. Mauri, N.L. Nguyen, H.-V. Nguyen, A. Otero-de-la Roza, L. Paulatto, S. Poncé, D. Rocca, R. Sabatini, B. Santra, M. Schlipf, A.P. Seitsonen, A. Smogunov, I. Timrov, T. Thonhauser, P. Umari, N. Vast, X. Wu, S. Baroni, J. Phys.: Condens. Matter 29 (46) (2017) 465901, http://dx.doi.org/10.1088/1361-648X/aa8f79, URL http://stacks.iop.org/0953-8984/29/i=46/a=465901?key=crossref.1e5990a1bce3cf815cc9651e7e95dbd2.

[7] N.A.W. Holzwarth, A.R. Tackett, G.E. Matthews, Comput. Phys. Commun. 135 (2001) 329–347, available from the website http://pwpaw.wfu.edu.

[8] G. Kresse, D. Joubert, Phys. Rev. B 59 (1999) 1758–1775.

[9] J.P. Perdew, Y. Wang, Phys. Rev. B 45 (1992) 13244–13249.

[10] J.P. Perdew, K. Burke, M. Ernzerhof, Phys. Rev. Lett. 77 (1996) 3865–3868; Phys. Rev. Lett. 78 (1997) 1396 (erratum).

[11] J.P. Perdew, A. Ruzsinszky, G.I. Csonka, O.A. Vydrov, G.E. Scuseria, L.A. Constantin, X. Zhou, K. Burke, Phys. Rev. Lett. 100 (13), http://dx.doi.org/10.1103/PhysRevLett.100.136406, URL https://link.aps.org/doi/10.1103/PhysRevLett.100.136406.

[12] S. Lehtola, C. Steigemann, M.J. Oliveira, M.A. Marques, SoftwareX 7 (2018) 1–5, Note that this analysis applies to functionals through the level of the generalized gradient approximation (GGA); further considerations will be needed for meta-GGA formulations. http://dx.doi.org/10.1016/j.softx.2017.11.002, URL http://linkinghub.elsevier.com/retrieve/pii/S2352711017300602.

[13] S.G. Louie, S. Froyen, M.L. Cohen, Phys. Rev. B 26 (1982) 1738–1742.

[14] Note that it is assumed that any overlap of core densities from different sites is negligible.

[15] D. Vanderbilt, Phys. Rev. B 41 (1990) 7892–7895, USPP code is available from the website http://www.physics.rutgers.edu/dhv/uspp/.

[16] K. Laasonen, R. Car, C. Lee, D. Vanderbilt, Phys. Rev. B 43 (1991) 6796–6799.

[17] K. Laasonen, A. Pawquarello, R. Car, C. Lee, D. Vanderbilt, Phys. Rev. B 47 (1993) 10142–10153.

[18] G. Kresse, J. Furthmüller, Phys. Rev. B 54 (1996) 11169–11186, proprietary code available at the website https://www.vasp.at/, http://dx.doi.org/10.1103/PhysRevB.54.11169, URL https://link.aps.org/doi/10.1103/PhysRevB.54.11169.

[19] A. Dal Corso, Comput. Mater. Sci. 95 (2014) 337–350, http://dx.doi.org/10.1016/j.commatsci.2014.07.043, URL http://linkinghub.elsevier.com/retrieve/pii/S0927025614005187.

[20] F. Jollet, M. Torrent, N. Holzwarth, Comput. Phys. Comm. 185 (2014) 1246–1254.

[21] O.K. Andersen, Phys. Rev. B 12 (1975) 3060–3083.

[22] P. Blaha, K. Schwarz, G. Madsen, D. Kvasnicka, J. Luitz, *WIEN2k, An Augmented Plane Wave Local Orbitals Program for Calculating Crystal Properties (Karlheinz Schwarz, Techn. Universität Wien, Austria), 2001, ISBN:3-9501031-1-2,* http://www.wien2k.at.

[23] S. Baroni, S. De Gironcoli, A. Dal Corso, P. Giannozzi, Rev. Modern Phys. 73 (2) (2001) 515, URL http://journals.aps.org/rmp/abstract/101103/RevModPhys.73515.